

Fully interconnected, linear control for limit cycle walking

Joseph H Solomon¹, Martijn Wisse² and Mitra JZ Hartmann^{1,3}

Adaptive Behavior
18(6) 492–506
© The Author(s) 2010
Reprints and permissions:
sagepub.co.uk/journalsPermissions.nav
DOI: 10.1177/1059712310389624
adb.sagepub.com



Abstract

Limit cycle walkers are a class of bipeds that achieve stable locomotion without enforcing full controllability throughout the gait cycle. Although limit cycle walkers produce more natural-looking and efficient gaits than bipeds that are based on other control principles such as zero moment point walking, they cannot yet achieve the stability and versatility of human locomotion. One open question is the degree of complexity required in the control algorithm to ensure reliable terrain adaptation and disturbance rejection. The present study applies a fully interconnected, linear controller to a two-dimensional, five-link walking model, achieving stable and efficient locomotion over unpredictable terrain (slopes varying between 2° and 7° and step-downs varying between 0 and 25% leg length). The results indicate that elaborate control principles are not necessarily required for stable bipedal walking.

Keywords

Dynamic walking, biped, disturbance rejection, reactive control, reflexive control, genetic algorithm

1 Introduction

Bipedal walking is a particularly well-studied form of locomotion because it is relevant to a wide variety of disciplines, including gait rehabilitation, computer animation, and entertainment and service robots. Since the 1990s computer simulations and robotic models have often been used to investigate the dynamics and control principles involved in human gait. The increasing recognition of the fundamental role played by passive dynamics has led to particularly elegant and simple control methodologies for these models (Collins & Ruina, 2005; Hobbelen & Wisse, 2008a, 2008b, 2008c, 2009, 2010; Kuo, 1999, 2002; Wisse, 2005; Wisse, Schwab, van der Linde, & van der Helm, 2005).

The pioneering work of Tad McGeer in the late 1980s showed that remarkably lifelike bipedal locomotion is possible without the aid of a single sensor or actuator (McGeer, 1990). McGeer simulated and carefully constructed simple two-legged machines that could walk down a shallow ramp by settling into a stable limit cycle, a process called *passive dynamic walking*. This concept fits into the more general paradigm recently termed *limit cycle walking*, wherein sensing and

actuation may be included in the synthesis of the gait pattern (Hobbelen & Wisse, 2007).

The design of control frameworks for limit cycle walkers is challenging in the sense that the dynamics are highly nonlinear, high-dimensional, and discretely changing, and because foot–ground contact is fundamentally underactuated (Pratt, 2000). On the other hand, McGeer's work showed that the natural dynamics of bipedal systems possess an inherent tendency toward *cyclic*, or *orbital* stability, which clearly simplifies the control task (Hobbelen & Wisse, 2007; McGeer, 1990; Strogatz, 2000).

Addressing this apparent contradiction, this article shows that simple linear control structures are sufficient for robust and efficient control of a two-dimensional

¹Department of Mechanical Engineering, Northwestern University, USA.

²Department of Mechanical Engineering, Delft University of Technology, The Netherlands.

³Department of Biomedical Engineering, Northwestern University, USA.

Corresponding author:

Joseph H. Solomon, Northwestern University, Department of Mechanical Engineering, 2145 Sheridan Road, Evanston, IL 60208, USA
Email: joe-solomon@northwestern.edu

(2-D), five-link walking model. By tuning the control parameters (connection weights) using an evolutionary algorithm (EA), the model is able to adapt to varying terrain slopes and recover from large step-downs, thus possessing surprising robustness for such a simple control architecture.

1.1 Motivation

The behavior of any embodied agent—whether an animal, a robot, or a simulated entity—can be viewed as emerging from the highly interdependent interactions between brain, body, and environment (Beer, 1995). In general, all three of these components can have dynamic properties; for example, for an animal, neurons possess a variety of continuously changing internal states, and both the body and environment move and react according to the classical laws of physics. Importantly, however, complex behaviors can emerge even for simple “reactive” agents situated in static environments, for which the control policy (nervous system) is a fixed, direct mapping between sensors and actuators.

This principle was superbly demonstrated by Valentino Braitenberg in his 1984 book *Vehicles: Experiments in Synthetic Psychology*. The book describes a series of 14 hypothetical two-wheeled vehicles equipped with various sensors (e.g., light, temperature, distance, etc.) with increasingly elaborate control rules, resulting in increasingly sophisticated behaviors. The elegance of Braitenberg’s exposition has led to many implementations of these principles in hardware, both for educational purposes and research. One particular study implemented a variant of Braitenberg’s Vehicle 3c on a Khepera mobile robot, equipped with eight proximity sensors emerging at various angles, setting each wheel’s speed command proportional to the weighted sum of sensor signals. Using an EA to tune the weights, the robot was successfully trained to navigate smoothly around a small track with frequent sharp turns (Mondada & Floreano, 1995).

Although a fully interconnected, linear (FIL) control scheme has produced interesting behaviors in mobile robots, to our knowledge no study has shown it to be viable for stable locomotion control. Instead, most approaches use significantly more elaborate control schemes that rely on internal states, such as desired joint angles, gait phase information or artificial neuronal activation. For example, in a series of highly influential studies, Taga applied neurophysiologically inspired central pattern generator (CPG)-based control models to various five-link walking models, commenting that “‘global entrainment’ between the neural and musculo-skeletal systems generates stable and flexible

locomotion in an unpredictable environment” (Taga, Yamaguchi, & Shimizu, 1991; Taga, 1995a). The models were able to recover from perturbations and adapt to varying surface slopes. However, the utility of the “global entrainment” allowed by the internal states of CPGs in the domain of limit cycle walking is not entirely clear.

Here, we show that the simple and elegant nature of purely reactive, linear control is sufficient to allow both robust terrain adaptation and disturbance rejection for a 2-D model of bipedal locomotion. Using an appropriate choice for the encoding of sensory variables, effective connection weights are consistently evolved using an EA. The best-performing control architecture presented here could reasonably be described as a *fully interconnected, multi-input-multi-output linear controller*. However, unlike a traditional feedback controller, there is *no explicit reference trajectory that is being tracked*. Instead, stable locomotion emerges as the EA searches for connection weights that *achieve a desired behavior*, namely stable and efficient locomotion.

1.2 Related Work

Previous research into the control of bipedal walking can be divided into two main categories: zero moment point (ZMP) and limit cycle walking. The ZMP control paradigm was established in the early 1970s by Miomir Vukobratović (Vukobratović & Borovac, 2004). ZMP refers to the point of contact between the foot and the ground about which the total contact force causes no moment (equivalent to the center of pressure when the feet are flat on the ground). In general, stability is accomplished by predefining a desired trajectory through state space which causes the ZMP to remain well inside the foot edges. This allows continuous full controllability around the predefined trajectory. The benefit is that standard feedback control can be used, but the drawback is that it requires stiff actuation, resulting in poor energy efficiency and unnatural-looking gait patterns. It is worth noting, however, that nearly all state-of-the-art humanoid robots (e.g., Honda’s ASIMO, Sakagami et al., 2002; Kawada Industries’ HRP-3P, Akachi et al., 2005; Sony’s QRIO, Ishida, 2004) currently incorporate some form of ZMP-based control.

The paradigm of limit cycle walking removes the full controllability constraint inherent in the ZMP approach, and emphasizes passive dynamics as the primary influence of the overall walking motion (Hobbelen & Wisse, 2007). Instead of using stiff actuators to track a rigidly defined trajectory, limit cycle walkers rely on “cyclic stability” or “orbital stability” (Strogatz, 2000), wherein neighboring trajectories converge over several steps to a nominal trajectory.

The resulting gait patterns are remarkably natural-looking and efficient, making limit cycle walking a highly effective approach to the synthesis of controllers for bipedal robots. The remainder of this section will review some of the most relevant publications on limit-cycle-walking-based walking controllers, with a particular focus on the use of EAs.

Early research on limit cycle walking in the early 1990s followed McGeer's initial studies, focusing mainly on passive dynamic walking (no sensing or actuation; e.g., Garcia, Chatterjee, Ruina, & Coleman, 1998; Goswami, Espiau, & Keramane, 1996). Based on principles learned from these studies, Collins and Ruina (2005) then constructed a fully 3-D limit cycle walking robot that used ankle push-off actuation to achieve a specific mechanical cost of transport (a measure of energy efficiency) approximately equal to that of humans. Research by Art Kuo was instrumental in introducing ways to actuate (Kuo, 2002) and incorporate feedback control (Kuo, 1999) for stable level-ground walking.

The Delft Biorobotics Laboratory has focused on developing methods to generate efficient limit cycle walking performance with good disturbance rejection, including swing leg retraction near the end of a step (Hobbelen & Wisse, 2008c), local stance ankle control and ankle push-off modulation ((Hobbelen & Wisse, 2008a), a combination of feedforward and feedback control to keep the body upright (Hobbelen & Wisse, 2010), increasing walking speed (Hobbelen & Wisse, 2008b), and a linear, lateral foot placement strategy (Hobbelen & Wisse, 2009). Chevallereau et al. (2003) used the concepts of "hybrid zero dynamics" and "virtual constraints" on the 2-D physical prototype RABBIT to achieve exponentially stable walking control. Several studies have applied reinforcement learning to limit cycle walking control in various ways, both in simulation (Chew & Pratt, 2002; Schuitema, Hobbelen, Jonker, Wisse, & Karssen, 2005) and in hardware (Tedrake, Zhang, & Seung, 2004). Byl and Tedrake (2009) investigated the "stochastic stability" of rimless-wheel and compass-gait walking models on rough terrain, and use tools from numerical stochastic optimal control to design controllers that maximize stochastic stability. Following the influential work of Taga (Taga et al., 1991), CPGs have also been commonly applied both in simulation and hardware (Endo, Morimoto, Nakanishi, & Cheng, 2004). Manoonpong, Geng, Kulvicius, Porr, and Wörgötter (2007) applied a hierarchical neural network control architecture with online learning mechanisms to a 2-D robot, RunBot, demonstrating fast and efficient walking performance with the ability to adapt to varying terrain slopes. Notably relevant to the present research, Ono, Takahashi, and Shimada (2001) studied

a simple control mechanism wherein the hip torque is directly proportional to knee angle and the knee joint is linearly damped, achieving stable walking with a 2-D biped on a shallow slope.

Evolutionary algorithms—a significant component of the approach taken here—have most typically been applied for control of multi-legged agents (Beer & Gallagher, 1992); relatively few studies have applied them to bipedal limit cycle walking control. Reil and Husbands (2002) used a genetic algorithm to tune the parameters of a fully connected continuous time recurrent neural network (CTRNN)—a form of CPG—for feedforward control of a simulated 3-D biped. Vaughan, Di Paolo, and Harvey (2004) evolved the parameters of a somewhat more elaborate continuous time neural network structure for control of a simulated 3-D biped, and found the resulting gait to be robust to external forces and changes in body parameters. McHale and Husbands (2004) compared performance of three different types of evolved neural networks on a 2-D simulated biped—a CTRNN, a plastic neural network (PNN), and a GasNet—finding that only the GasNet was able to achieve cyclical locomotion. Most similar to the present study, Paul (2005) evolved the connection weights of simple linear feedforward neural networks to control the gait of a simulated 3-D biped. Linearly weighted connections from all joint angle sensors, a binary foot contact sensor, and a bias were fed into PD controllers, which output torque signals for the ankle, knee, sagittal hip, and frontal hip actuators. The controller was able to produce a gait pattern over level terrain, although the step lengths were unusually short. The most significant differences between Paul's work and that presented here is that this study incorporates velocity state information, and we demonstrate efficient locomotion with the ability to adapt to varying slopes and recover from large step-downs.

2 Methods

2.1 Biped Model

The 2-D, five-link biped model used in this study is shown in Figure 1. It is equipped with sensors measuring stance and swing knee angles $\phi_{k,st}$ and $\phi_{k,sw}$, stance and swing thigh segment angles with respect to the upper body $\phi_{h,st}$ and $\phi_{h,sw}$, and upper body angle with respect to gravity ϕ_b . One of our controllers made use of the inter-leg angle between the two thigh segments, defined as ϕ_{il} , equal to the sum of $\phi_{h,st}$ and $\phi_{h,sw}$. Actual parameter values are given in Table 1. Although it is common to include arc-shaped feet or ankle springs in

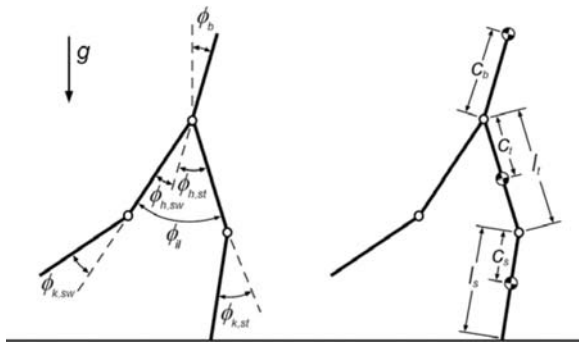


Figure 1. Five-link walking model. Left: angle definitions. Right: length definitions.

Table 1. Parameter values for five-link walking model. The body length is not provided because it plays no role in the biped's dynamics; only the center of mass is relevant

	body	thigh	shank
mass, m [kg]	5	2	1
length, l [m]	–	0.3	0.3
center of mass, c [m]	0.2	0.1	0.1
moment of inertia, I [kg·m ²]	0.15	0.02	0.01

limit cycle walking models and robots for improved energy efficiency and disturbance rejection capabilities (Hobbelen & Wisse, 2007; Wisse, Hobbelen, Rotteveel, Anderson, & Zeglin, 2006), this was not done here in order to increase the difficulty of the control problem.

The dynamics of this model consists of a continuous swing phase during which the swing leg smoothly swings past the stance leg, and an instantaneous, fully inelastic heel strike when the swing foot touches the floor. We do not model a double stance phase. Instead, the swing foot is assumed to leave the floor at the instant of heel strike, and we monitor the validity of this assumption by checking whether the postimpact velocity vector of the swing foot is indeed pointing above the terrain. The swing leg knee contains a hyper-extension stop and a latch that is activated upon full extension to hold the leg straight; the latch remains active during the stance phase and is released at the start of the subsequent swing phase. All simulations were performed using a Matlab's fourth- and fifth-order variable time-step Runge-Kutta solver (ode45, Revision 5.74.4.4, with relative error tolerance set to 10^{-12}). Each time heel strike or full knee extension occurs, the solver is stopped, an impact calculation is performed, and the solver is started again with the new initial conditions. This is a standard approach in modeling dynamic systems to perform discrete impact calculations.

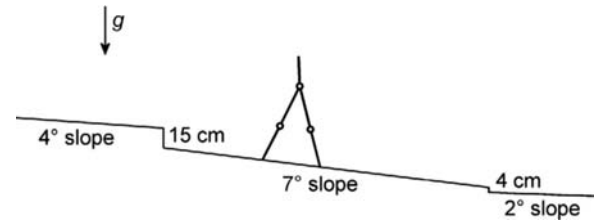


Figure 2. The terrain model includes both discretely changing surface slopes and abrupt step-downs.

2.2 Terrain Model

The objective is to test the capability of the control scheme to adapt to varying terrain conditions and to reject abrupt disturbances, while simultaneously expending as little energy as possible. The terrain model thus consists of a series of straight segments of randomly varying surface slope, between which abrupt drops in terrain height occur. Specifically, every 2–4 m, a step-down of 0–15 cm occurs, and the slope is changed to a value between 2° and 7° (all three values from uniform random distributions). The changing surface slopes test the ability of the biped to transition into stable limit cycles that are appropriate for the current terrain conditions, which we consider *terrain adaptation*, while at the same time recover from large perturbations in the form of step-downs, which we consider *disturbance rejection*. Part of a typical section of terrain is shown in Figure 2. The reason for ensuring that the floor slope remains steeper than 2° is to allow energy lost from heel strike impacts to be replenished by gravity, as we do not model ankle push-off and keep the stance leg fully-extended. This is typical for simulations of limit cycle walking (Garcia et al., 1998). Also note that the swing foot is allowed to pass through the previous terrain segment after a step-down, as the discrete contact model would otherwise interpret an impact as occurring immediately following large step-downs.

2.3 Neural Network Models

We refer to the controllers as neural networks, specifically feedforward, two-layer neural networks with sigmoid (tanh) transfer functions. Thus, they are identical to classical perceptrons, except the transfer functions are sigmoids instead of threshold functions.

There are a total of four control torques on the biped model: $\tau_{k,st}$ at the stance knee, $\tau_{k,sw}$ at the swing knee, $\tau_{h,st}$ at the stance hip (between the stance leg and the upper body), and $\tau_{h,sw}$ at the swing hip (between the swing leg and the upper body). The two torques for the swing leg are implemented with neural networks, while the two torques for the stance leg are

Table 2. Neural network models

Model	Description	Activations
1	Inter-leg PD control	$a_{h,sw} = w_1 \dot{\phi}_{il} + w_2 \phi_{il} + w_3$ (3)
		$a_{k,sw} = w_4 \dot{\phi}_{k,sw} + w_5 \phi_{k,sw}$ (4)
2	Swing thigh PD control	$a_{h,sw} = w_1 \dot{\phi}_{h,st} + w_2 \phi_{h,sw} + w_3 \dot{\phi}_{h,sw} + w_4$ (5)
		$a_{k,sw} = w_5 \dot{\phi}_{k,sw} + w_6 \phi_{k,sw}$ (6)
3	Fully interconnected, linear (FIL)	$a_{h,sw} = w_1 \dot{\phi}_{h,st} + w_2 \phi_{h,sw} + w_3 \dot{\phi}_{k,sw} + w_4 \dot{\phi}_{h,st} + w_5 \dot{\phi}_{h,sw} + w_6 \dot{\phi}_{k,sw} + w_7$ (7)
		$a_{k,sw} = w_8 \dot{\phi}_{h,st} + w_9 \phi_{h,sw} + w_{10} \dot{\phi}_{k,sw} + w_{11} \dot{\phi}_{h,st} + w_{12} \dot{\phi}_{h,sw} + w_{13} \dot{\phi}_{k,sw} + w_{14}$ (8)
4	FIL, no knee torque	$a_{h,sw} = w_1 \dot{\phi}_{h,st} + w_2 \phi_{h,sw} + w_3 \dot{\phi}_{k,sw} + w_4 \dot{\phi}_{h,st} + w_5 \dot{\phi}_{h,sw} + w_6 \dot{\phi}_{k,sw} + w_7$ (9)
		$a_{k,sw} = 0$ (10)

implemented with fixed gain proportional-derivative (PD) controllers. The motivation and details of this simple architecture will now be explained.

Limit cycle walkers typically fully extend the swing leg at the end of the swing phase and keep it fully extended throughout the stance phase (Wisse et al., 2005). In such cases, no stance knee control is necessary. However, there may be instances when full swing leg extension does not occur, for example following a step-down, due to the excess forward rotational velocity of the stance leg. To accommodate for such cases, a PD controller (with a set point of 0°) is implemented on the stance leg:

$$\tau_{k,st} = k_{p,knee} \phi_{k,st} + k_{d,knee} \dot{\phi}_{k,st} \quad (1)$$

with $k_{p,knee} = 100 \text{ N}\cdot\text{m}$ and $k_{d,knee} = 5 \text{ N}\cdot\text{m}\cdot\text{s}$.

A PD controller was also implemented for the upper body. Because humans tend to walk with their upper bodies nearly fully upright, within $\pm 1^\circ$ in the sagittal plane (Winter, 1991), and this strategy has proven effective in other limit cycle walking simulations and robots (Hobbelen & Wisse, 2010), the set point is set to coincide with the direction of gravity, yielding:

$$\tau_{h,st} = k_{p,body} \phi_b + k_{d,body} \dot{\phi}_b - \tau_{h,sw} \quad (2)$$

with $k_{p,body} = 100 \text{ N}\cdot\text{m}$ and $k_{d,body} = 5 \text{ N}\cdot\text{m}\cdot\text{s}$. This torque is exerted at the hip with respect to the stance leg, which switches between sides after each heel strike. Notice that in Equation 2, the quantity $\tau_{h,sw}$ is subtracted from the PD components. This was done because both $\tau_{h,st}$ and $\tau_{h,sw}$ act on the upper body. Subtracting $\tau_{h,sw}$ effectively isolates control of the swing leg from control of the upper body.

For the remaining two actuators, controlling $\tau_{k,sw}$ and $\tau_{h,sw}$, the control architectures investigated here are simple weighted linear mappings from sensor states to motor torques. We investigate four variants of this concept, listed in Table 2.

In Table 2, a is the activation of the corresponding “neuron” and w_1 through w_{14} are the neural network weights. All state variables were affinely transformed to the range $[-1, 1]$ using the procedure outlined in the Appendix. In order to enforce limits on the motor torques, each neural network output passes through a sigmoid in the form of the hyperbolic tangent function, limiting the output range to $[-1, 1]$. The final output torques are given by

$$\tau_{h,sw} = \tau_{h,sw,max} \tanh(a_{h,sw}) \quad (11)$$

$$\tau_{k,sw} = \tau_{k,sw,max} \tanh(a_{k,sw}) \quad (12)$$

where $\tau_{h,sw,max}$ and $\tau_{k,sw,max}$ were given values of $5 \text{ N}\cdot\text{m}$ and $1 \text{ N}\cdot\text{m}$, respectively, which are modest maximum values for a robot of this size. The justification for investigating these particular neural network structures will now be explained.

Model 1 simply incorporates PD controllers on the hip and knee joints, and makes use of the inter-leg angle ϕ_{il} , described earlier as the angle between the two thigh segments:

$$\phi_{il} = \phi_{h,st} + \phi_{h,sw} \quad (13)$$

Note that although Equation 3 does not take the traditional form of a PD controller, it can easily be converted to one by substituting $k_p = w_1$, $k_d = w_2$, and $\theta_{setpoint} = -w_3/w_1$. Hence, Equation 3 will simply cause the swing leg to travel to the effective set point. Because Equation 4 has no bias term, the set point is zero degrees (full knee extension). PD control laws such as these have proven effective in previous limit cycle walking simulations and robots (Wisse, 2005; Wisse et al., 2005). Thus, Model 1 serves as a reasonable performance benchmark. Also, including superfluous inputs can detrimentally affect machine learning techniques (cf., Paul, 2005), so it is possible that Model 1 could outperform the others, despite incorporating less state information.

Model 2 is very similar to Model 1, except it maintains $\phi_{h,st}$ and $\phi_{h,sw}$ as separate variables instead of summing them into ϕ_{il} . Because the upper body remains relatively upright, independently expressing these two variables effectively provides information about the orientation of the stance leg relative to gravity. Model 2's swing leg control can still be thought of as a PD controller, but now applied to the absolute swing thigh angle (instead of inter-leg angle), and the set point dynamically changing (a linear function of $\phi_{h,st}$), and uses $\dot{\phi}_{h,sw}$ instead of $\dot{\phi}_{il}$.

Model 3 represents FIL control, wherein weighted values of all raw sensor states (and a bias) are linearly summed to form the network activations. Although several of these connections have no intuitively obvious control utility, this model tests the possibility that they confer some emergent control benefit.

Model 4 has the identical hip torque to Model 3, but there is no swing knee actuation. This model is thus used to investigate the necessity of swing knee actuation for this control task.

2.4 Evolutionary Robotics

Evolutionary robotics is a method of applying the principles of natural selection to the development of robotic systems, or most commonly to the synthesis of robotic control systems (Stefano & Floreano, 2000). In practice, this generally means that some form of EA (Eiben & Smith, 2003) is used to search the parameter space of a control structure to produce the behaviors that best carry out a desired task. In the present work, we used a form of EA most similar to the branches of *evolutionary programming* and *evolution strategies*, as described below.

The fitness function (performance metric) to be optimized by the EA was chosen to be the horizontal distance d traveled before the walker expends a fixed amount of energy ($W_0 = 200$ Joules) or falls down. (Note that *optimization* is of course only the idealized goal, not the expected outcome.) The mechanical work generated by the actuators can be computed using

$$W = \sum_{i=1}^4 \int_0^T |\tau_i \cdot \dot{\phi}_i| \cdot dt \quad (14)$$

where ϕ_i and τ_i refer to the angles and corresponding actuators defined in Figure 1 (left) ($\tau_{h,st}$, $\tau_{h,sw}$, $\tau_{k,st}$, $\tau_{k,sw}$), and T is the total time elapsed since the start of the trial. The justification for this fitness function is that it effectively optimizes for both stability and efficiency: fitness can only be high if the biped doesn't fall down (stable), and is frugal with its limited store of energy

(efficient). Another implicit benefit is that in early generations energy efficiency does not play a vital role—because most individuals will only take a few steps at most—and hence the selection pressure is for a stable gait, while in later generations selection pressure toward energy efficiency also becomes a significant factor. Each fitness evaluation starts with the biped taking a step forward using the hand-selected initial conditions shown in Table 3.

To decrease the computation time for fitness function evaluations, an evaluation was terminated once the biped took a step past $d_{max} = 20$ m, and the fitness f was scaled according to the amount of energy expended, such that

$$f = \begin{cases} d, & d \leq d_{max} \\ d \cdot \frac{W}{W_0}, & d > d_{max} \end{cases} \quad (15)$$

Each run of the EA starts with a population of 100 random genotypes, with each gene encoding a single weight as a real number, randomly and uniformly initialized in the range $[-1, 1]$. After all genotypes are evaluated, 20 of them (as explained in the next paragraph) are copied five times and mutated by adding a vector of normally distributed random numbers with zero mean and a standard deviation ranging between 0.2 and 0.05 (0.2 for the first generation, linearly decreasing to become 0.05 on the last). No limits are enforced on the ranges of the resulting genes (i.e., weights). Each run lasted 100 generations, and 20 runs were performed for each of the four models.

A form of age-based elitism was used to help allay the effects of noisy fitness function evaluations, caused by the random regeneration of terrain each generation. The single fittest individual of each generation automatically survives for five additional generations. As a result, generations $g = 0$ through 4 (where $g = 0$ is the initial random population) were generated using g elite individuals from previous generations, and the best $20 - g$ non-elite from the preceding generation. Similarly, generations $g = 5$ through 100 were generated using five elite individuals from previous

Table 3. Initial conditions used in walking trials

ϕ_b [rad]	$\phi_{h,st}$ [rad]	$\phi_{h,sw}$ [rad]	$\phi_{k,st}$ [rad]	$\phi_{k,sw}$ [rad]
0	$\pi/16$	$\pi/16$	0	0
$\dot{\phi}_b$ [rad/s]	$\dot{\phi}_{h,st}$ [rad/s]	$\dot{\phi}_{h,sw}$ [rad/s]	$\dot{\phi}_{k,st}$ [rad/s]	$\dot{\phi}_{k,sw}$ [rad/s]
0	$-\pi/3$	$-\pi/3$	0	$-\pi$

generations, and the best 15 non-elite from the preceding generation.

To evaluate the performance of each run, an overall “winner” is selected at its completion. Because of the noisy fitness evaluations, the fittest individual of the last generation would not necessarily be the best overall performer for random terrain. Therefore, a tournament was held using the fittest individuals from the last 20 generations. Each was evaluated 20 times, and the one with the best average fitness was declared the winner. Finally, the winner was evaluated 100 times on newly generated terrain segments to accurately measure its fitness.

3 Results

The results of each of the 20 runs for each of the four models are shown in Figure 3a–d. Figure 3e indicates the results for the four models averaged over the 20 runs.

The local joint PD control architecture of Model 1 did not evolve stable controllers. To help determine why, we conducted an additional run with Model 1 that involved no step-downs, and the tournament winner fell on 57% of the test runs. Hence, the local joint-level PD control technique of Model 1 was able to accommodate for about 95% of the changes in surface slope, but completely unable to accommodate for the step-downs. Interestingly, the stance leg orientation information used in Model 2 overcame this limitation, and stable walking became possible. The FIL architecture of Model 3 was the best performer of all, consistently evolving walking controllers that were both stable and efficient. Model 4 shows that swing knee actuation is not necessary for robust control under the current terrain model, quickly evolving good walking controllers; however, Figure 3e indicates that although Model 3 is slower to optimize the larger number of control weights, superior results can be eventually achieved. Indeed, unlike the others, Model 3 was

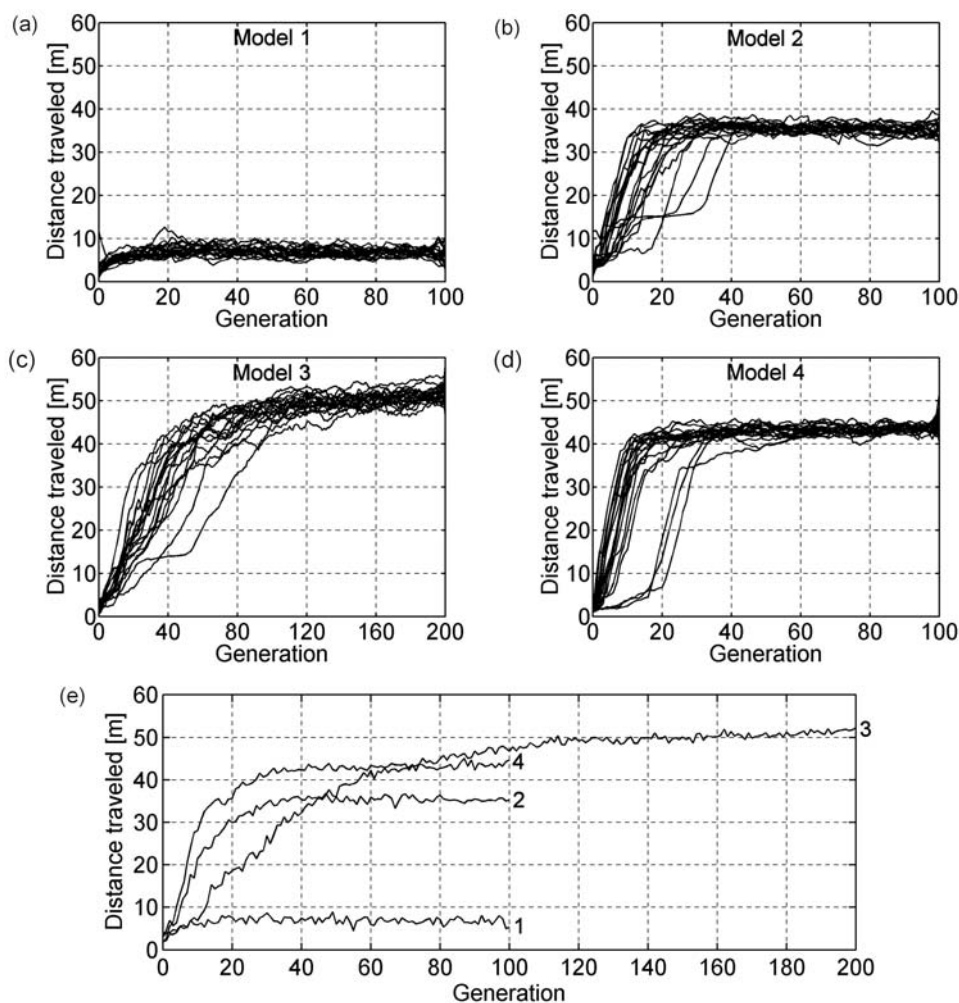


Figure 3. Evolutionary algorithm results. (a–d) Individual results of 20 evolutionary runs of Models 1 to 4, each smoothed using a nine-point moving average. (e) Overall averaged results of Models 1 to 4.

continuing to improve at the 100th generation. This slower rate of convergence can simply be attributed to larger number of weights being optimized.

The fact that Models 2 to 4 consistently evolved stable controllers indicates favorable underlying fitness landscapes. In other words, the geometric shapes of the mappings (hypersurfaces) from weight space to fitness enable quick and consistent optimization by the EA, because they contain numerous regions where gradients can be followed to regions of high fitness. Any local optima are small enough to be “escaped” via the mutation operator. This is an important property, as researchers evolving locomotion controllers oftentimes encounter the *bootstrap problem*, meaning that the EA is unable to progress beyond a very low fitness (i.e., unable to find a gradient to start descending; Beer & Gallagher, 1992; Reil & Husbands, 2002; Stefano & Floreano, 2000).

Figure 3e illustrates only the maximum distance traveled versus generation, averaged over the 20 runs. However, the quantity that we actually seek to maximize is the typical distance traveled over random terrain for the best individual from each run. Figure 4 therefore shows results of the final tournaments held at the end of each run of the EA.

Figure 4a shows that the curves in Figure 3 are a reasonable approximation to the ultimate performance of each model, with Model 3 performing the best, followed by Models 4, 2, and 1. Figure 4b shows the fraction of runs that end in a fall, as opposed to running out of energy or reaching the limit of 20 m. Model 3 consistently evolved highly stable controllers, with the 11 of the tournament winners falling at most once over the 20 test runs. Hence, Model 3 is superior to (*strictly dominates*) the others in terms of efficiency and stability.

Interestingly, although Model 4 generally leads to slightly greater walking distances than Model 2

(i.e., achieved better results with respect to the fitness function), it also falls down slightly more frequently, and so can be considered more efficient but less stable. A total of seven of Model 2’s tournament winners did not fall over the 100 test runs, compared with only one for Model 4. One easy way to encourage the evolution of more stable controllers would be to increase W_0 and d_{max} (d_{max} can be infinity), causing individuals to be tested over a longer stretch of terrain (but at the cost of slower fitness evaluations).

To gain some insight into how the controllers work, Figure 5 plots the average weights that evolved over the 20 runs for each model, along with their standard deviations.

In general, the standard deviations in Figure 5 are relatively small compared with the overall range in weight values. This indicates that the models’ underlying fitness landscapes are macroscopically unimodal in shape. In other words, there are likely not distantly spaced, high fitness local optima in the weight space. This is a favorable property in that any effective numerical optimization technique applied to these models will not produce significantly suboptimal results.

Since no stable controllers evolved for Model 1 (Figure 5a), there is little use in analyzing its weights.

Model 2 (Figure 5b) clearly makes primary use of only two sensory states (and a bias): $\phi_{h,sw}$ and $\dot{\phi}_{h,sw}$; both knee actuation weights averaged around zero and the weight for $\phi_{h,st}$ was about one-sixth that of $\phi_{h,sw}$ and $\dot{\phi}_{h,sw}$. To test whether stable locomotion is possible without $\phi_{h,st}$, an additional evolutionary run was undertaken, and stable controllers did not evolve. Thus, although the weight for $\phi_{h,st}$ was relatively small, this state is clearly providing critical information. This is an intuitive result, as a large stance leg angle is indicative of the occurrence of a step-down.

The weights of Models 3 and 4 are difficult to formally interpret due to the number of weights involved, although a few features are worth noting.

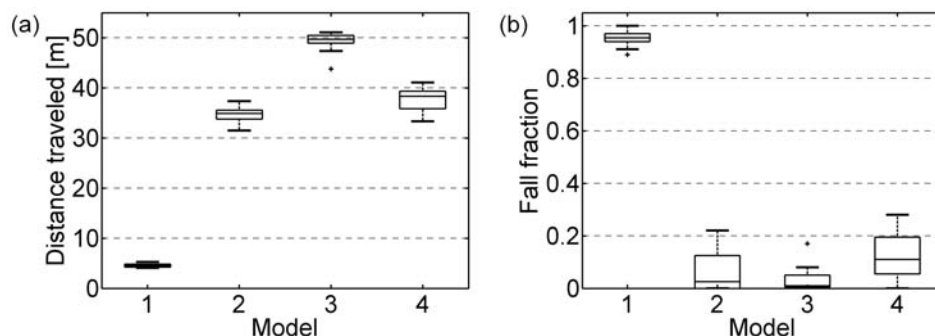


Figure 4. Results of the final tournaments held at the end of each EA run. (a) The boxplot shows the fitness (distance traveled) for the tournament winners of the 20 EA runs. (b) The fraction of runs that lead to falls for the tournament winners. Lower boundary, dividing line, and upper boundary indicate the lower quartile (Q1), median (Q2), and upper quartile (Q3), respectively. The “whiskers” are minimum and maximum. Data points outside $1.5 \cdot (Q_3 - Q_1)$ are considered outliers and are indicated by a + symbol.

The hip controllers for Models 3 and 4 (weights 1 through 7) converged to very similar values, indicating that the presence of knee actuation did not significantly alter that basic hip actuation strategy.

In contrast, the presence of additional weights for hip control in Models 3 and 4 compared with Model 2 did affect the values of weights associated with the state variables that they had in common.

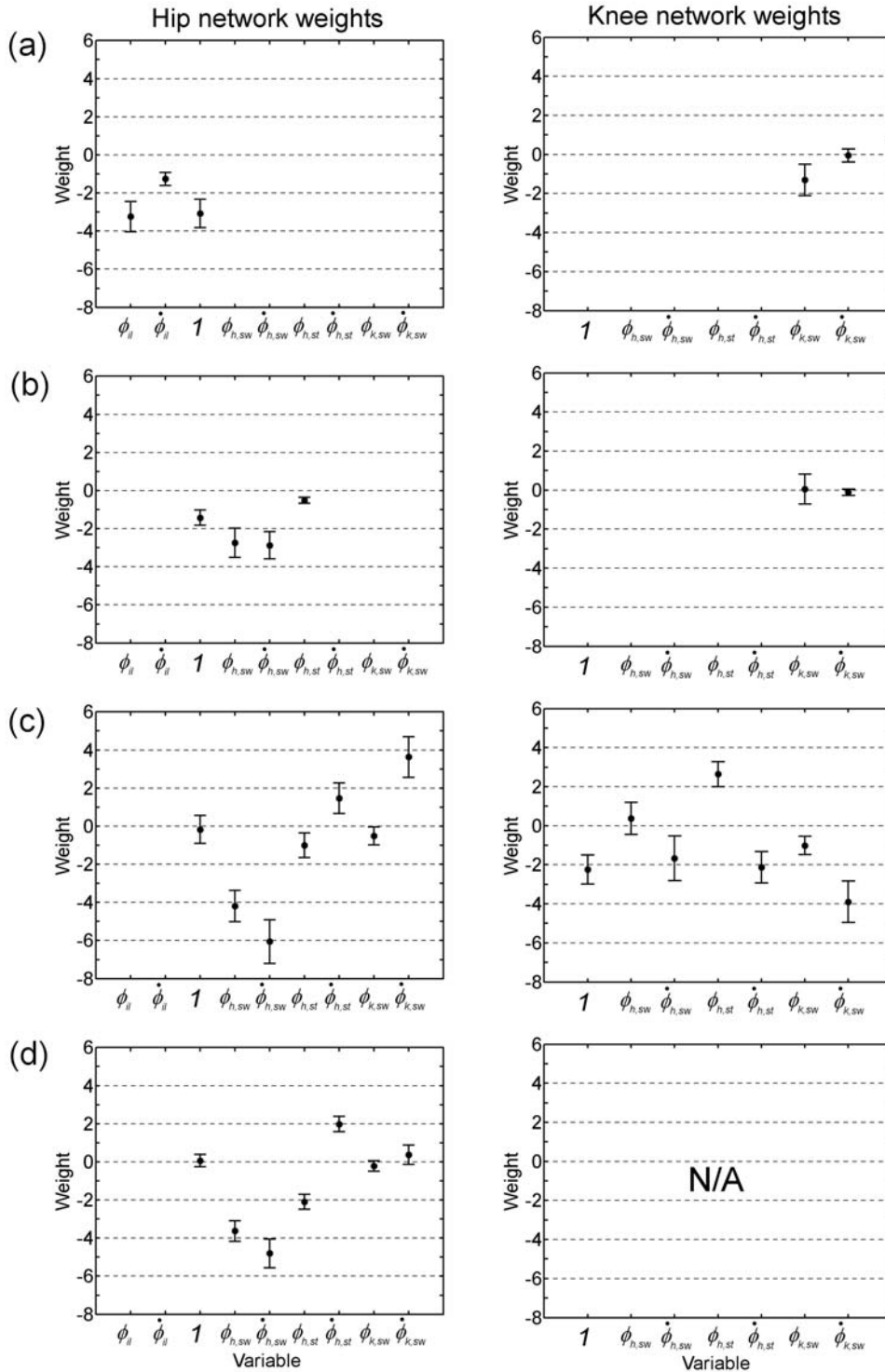


Figure 5. Average weight values of evolved controllers. Error bars indicate standard deviations. (a) to (d): Models 1 through 4. The “1” in the abscissa refers to the bias input.

To illustrate the basic control strategies employed by Model 3, Figure 6 shows the behavior of the biped transitioning from terrain with a slope of 2° to 7° , and after a step-down of 0.1 m. The weights of the fittest evolved controller were used, although most weights exhibited similar overall behavior. See accompanying animation online for an example of a full walking trial.

The torque signals for the swing hip and knee in the case of the step-down (Figure 6, bottom) are given in Figure 7a and b, respectively. It is clear that the hip actuation trajectory is very similar for both surface slopes. A brief but large negative torque abruptly increases the swing leg velocity at the beginning of each step, especially for the 2° slope. A small positive torque then slightly slows the swing leg down until knee-lock occurs, at which point a large torque serves to dampen out the effects of the knee impact, as can be seen in

Figure 6 (right). For the remainder of the step, a moderate negative torque keeps the swing leg extended forward. The step-down is basically handled by continued application of the negative torque, thereby increasing the swing leg velocity and the step width.

The roles of swing knee actuation are slightly more difficult to interpret. For the 2° surface slope, a step begins with a negative knee torque to increase $\dot{\phi}_{k,sw}$, while for the 7° slope, a positive torque slows it down. For both slopes, however, a positive torque is applied before knee extension, helping to reduce the effects of knee impact. After the step-down, a large positive torque helps to decrease $\dot{\phi}_{k,sw}$, consistent with the need to reduce the overall kinetic energy of the system.

All disturbances discussed thus far were in the form of abrupt step-downs. In order to test the ability of the model to recover from force perturbations (pushes),

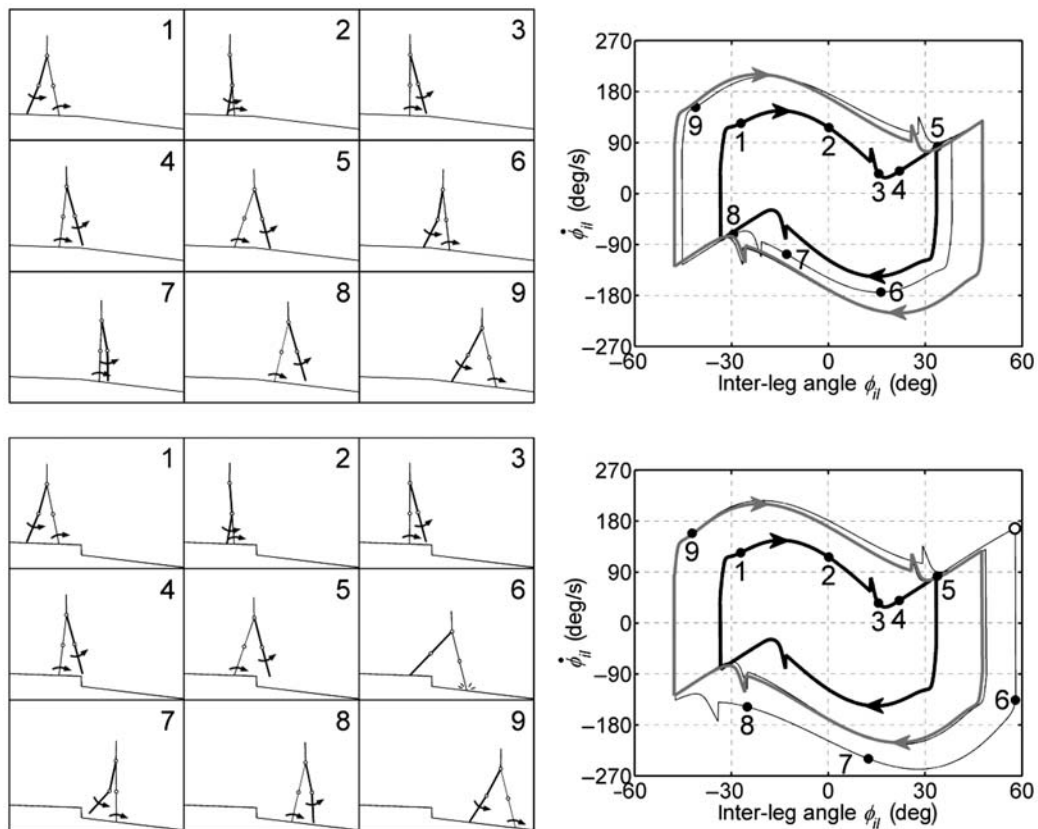


Figure 6. Response of the Model 3 biped to a change in ground slope from 2° to 7° , with (bottom) and without (top) a 0.1 m step-down. Left: Time elapsed between each frame is 0.2 seconds, and the first five frames are identical in both cases. Swing leg is indicated as a thick line. Right: Corresponding to each series of frames is the limit cycle between $\dot{\phi}_{il}$ and ϕ_{il} . The sign of both variables was reversed on even-numbered steps for clarity. Each numbered point on the limit cycle corresponds to a frame number. The thick black line is the limit cycle before the step-down, the thin black line is the transient response, and the thick gray line is the limit cycle after the step-down. When no step-down occurs, the biped gently settles into the new limit cycle within two steps (top-right). When a step-down does occur, $\dot{\phi}_{il}$ rapidly increases to increase the step length before heel-strike and thereby prevent excess kinetic energy from being added by the step-down (bottom-right). In the step that follows, the magnitude of $\dot{\phi}_{il}$ remains high as the swing leg quickly swings forward to prevent a fall from occurring. An example of the instantaneous state transition that occurs at heel strike is reflected by the distance between the small open circle and the state at frame 6 in the bottom-right graph.

additional simulations were performed. The perturbations were modeled as brief (0.1 s) horizontal forces at random locations along either the upper-body segment or the swing leg, with a 50% probability of either. The force magnitudes were between 10% and 40% of the total weight of the walker and occurred every 2–4 s during a trial, with both values picked from a uniform distribution. Model 3 was trained to reject the perturbations (along with the original changing slopes and step-downs) by running an additional 100 EA generations, starting at the last generation (i.e., 200) from the previous runs. A total of 20 additional runs were performed and, on average, the tournament winners fell on 62% of the runs. See accompanying animation online for an example of a successful walking trial with force perturbations. Examination of several runs revealed that the vast majority of falls were due to strong backwards pushes on the upper body, especially on shallow slopes, which prevented the walker from taking a step forward. Because of the discrete impact modeling technique used in the simulations (i.e., no double stance), it would be difficult or impossible for the controller to be able to compensate for these types of pushes.

4 Discussion

This study has developed and tested simple linear neural network models for robust control of limit cycle walkers. Stable, efficient and adaptable walking was evolved despite the simplicity of the control scheme. Previous research has suggested that a controller with internal rhythmicity (e.g., CPGs) may be necessary to adapt bipedal locomotion to a changing environment through “global entrainment” (Taga et al., 1991; Taga, 1995a,b). The present study casts some doubt as to the necessity of internal control states by showing that a linear, reactive framework is sufficient for stable, efficient and adaptable control of walking.

It was found that angle $\phi_{h,st}$ provides critical information to control hip torque for step-down recovery. Since the upper body was controlled so as to remain close to vertical and the stance knee is locked out, $\phi_{h,st}$ effectively represents the orientation of the stance leg. Thus, if Model 2 is viewed as a PD controller for the swing thigh angle, then its set point can be thought of as a linear function of the stance leg angle. When a step-down occurs, the stance leg angle increases. This in turn increases the effective set point angle and hence the step width, thereby enabling step-down recovery. This insight suggests a remarkably simple way to improve the step-down robustness of limit cycle walking robots that use controllers akin to Model 1, such as “Mike” and “Denise” of the Delft Biorobotics Laboratory (Wisse, 2005). More recently, Byl and Tedrake (2009) applied an inter-leg PD controller equivalent to that of Model 1, along with a fixed-magnitude, impulsive toe-off, to a compass gait biped model, enabling stable walking over rough terrain. However, using techniques from stochastic optimal control, their control policy actively modulated the inter-leg set point based on the state of the walker at the end of the preceding step. Thus, although their policy essentially makes use of the full state of the walker, certain states (e.g., stance leg velocity) are only accounted for on a step-to-step basis. This contrasts with the FIL architecture (Model 3), which is constantly monitoring all states.

Although the additional somewhat nonintuitive variables for hip torque control in Models 3 and 4, such as swing knee angle and velocity, are not necessary for stability, they do increase overall walking efficiency, and for most runs the stability as well. One possible interpretation for the increased efficiency is that evolving weights for $\phi_{k,sw}$ and $\dot{\phi}_{k,sw}$ effectively allows the EA to search amongst a wider variety of torque trajectories during steady state walking and step-down response, some of which are more efficient. Although knee

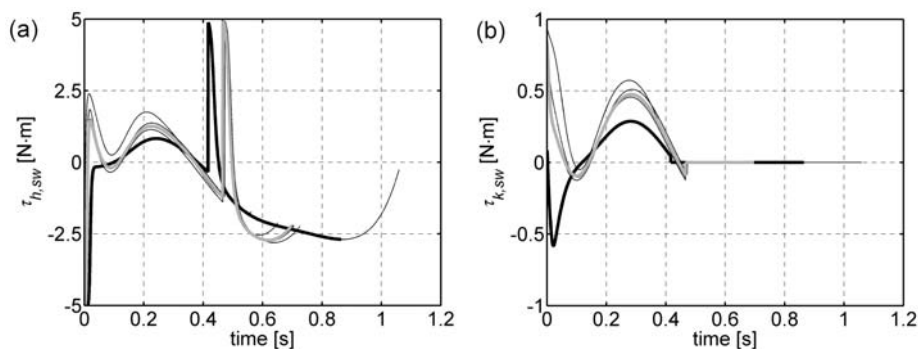


Figure 7. Swing hip torque (a) and swing knee torque (b) from walking on 2° (thick black lines) and 7° (thick gray lines) surface slopes. A 0.1 m step-down occurs between the change in slope, as shown in Figure 6 (lower-left). The transient response is indicated by the thin black line. After full knee extension occurs, a knee latch mechanism holds the swing leg straight and the torque stays at zero for the remainder of the step.

actuation is not absolutely necessary for stable locomotion, the EA more frequently evolved robustly stable controllers when knee actuation is allowed (see Figure 4). Also, comparing Models 3 and 4, using knee actuation led to more efficient controllers in all runs of the EA.

Future studies will likely benefit from a more elaborate upper-body controller than that used in this study (Hobbelen & Wisse, 2010). We did attempt to evolve fully interconnected upper-body controllers, but walking behavior did not emerge since the upper body always tended to quickly accelerate forward or backward and cause a fall. Hence, evolution could not get started, exhibiting the bootstrap problem mentioned earlier. This problem can likely be addressed by manually biasing the network weights for the upper-body controller in the initial population, for example, using weights that make the controller start out functionally equivalent to Equation 2, or by applying a sigmoid (“squashing”) function to the network output, that is, constraining it to a reasonable range (e.g., -10° to $+10^\circ$).

Because of the specific nature of the terrain model, it is difficult to directly compare the energy efficiency of the present simulations with that of humans or existing robots. However, to put the performance into some context, the dimensionless specific mechanical cost of transport is a convenient metric, computed by

$$c_{mt} = \frac{(\text{mechanical energy used})}{(\text{weight}) \cdot (\text{distance traveled})} \quad (16)$$

Using the median distances traveled from Figure 4a, the average c_{mt} for Models 2, 3, and 4 were 0.059, 0.038, and 0.054, respectively (note that this is a slightly conservative, i.e. high, value for Model 4 because the *distance traveled* is reduced by occasional falls). Studies have shown that humans walking on level ground have a c_{mt} of about 0.05, and existing limit cycle walking robots typically vary from about 0.02 to 0.07 (Collins, Ruina, Tedrake, & Wisse, 2005), both similar in efficiency to the present simulations.

Several issues stemming from this research remain to be investigated. The FIL control architecture should be adapted to a more realistic biped model, for example one that incorporates 3-D dynamics, a more elaborate terrain model, and a nondiscrete double stance phase. Two significant additional issues that arise here include lateral dynamics and stability issues, and the need for ankle push-off. Conveniently, both issues have already been addressed using simple linear control principles (Hobbelen & Wisse, 2008a, 2009), showing how straightforward extensions to the control architectures proposed here may allow extremely robust limit cycle walker control. To this end, we have recently

implemented a similar controller on 2-D and 3-D seven-link models (incorporating feet segments), successfully demonstrating push-off during double stance and the ability to walk over rough terrain. Although the simulation results are promising, transfer to hardware is needed to establish the real-world viability of FIL locomotion control. Hardware transfer represents a notorious challenge in the field of evolutionary robotics (Jakobi, Husbands, & Harvey, 1995).

5 Conclusion

As a relatively new research area in the field of bipedal robots, limit cycle walking invites the application and analysis of a variety of different control approaches. The FIL control scheme presented in this study indicates that linear control enables fundamental capabilities for limit cycle walking control: terrain adaptation, perturbation recovery, and energy efficiency. It should be noted, however, that the control framework used here significantly deviates from the conventions of traditional control theory, in that there is no explicit set point or reference value that is being regulated. Instead, stable locomotion emerges as the EA searches for weights that achieve a high level of fitness. It could be informally argued that FIL control probably lies near the Pareto frontier of performance versus complexity for limit cycle walking, meaning it would be difficult to construct a more stable and efficient controller without somehow increasing the complexity of the control structure (e.g., as measured by Kolmogorov complexity). At the very least, it reinforces the concept that although bipedal walking takes place in a high-dimensional state/action space, bipedal walking does not suffer from the “curse of dimensionality” (Bellman, 1957) from a control perspective.

Acknowledgments

This work was supported by the Office of Naval Research Award number N000140610218; and through the Director’s Research and Development Fund program of the Jet Propulsion Laboratory, California Institute of Technology to MJZH. M. Wisse was partially funded by the Dutch Technology Fund STW; and by the Commission of the European Union, within Framework Programme 6, RTD programme IST, under contract number FP6-2005-IST-61-045301-STP.

References

- Akachi, K., Kaneko, K., Kanehira, N., Ota, S., Miyamori, G., Hirata, M., et al. (2005). *Development of Humanoid Robot HRP-3P*. Paper presented at the Proceedings of the International Conference on Humanoid Robots.
- Beer, R. D. (1995). A dynamical systems perspective on agent–environment interaction. *Artificial Intelligence*, 72, 173–215.

- Beer, R. D., & Gallagher, J. C. (1992). Evolving dynamical neural networks for adaptive behavior. *Adaptive Behavior*, 1(1), 91–122.
- Bellman, R. E. (1957). *Dynamic programming*. Princeton, NJ: Princeton University Press.
- Bishop, C. M. (1996). *Neural networks for pattern recognition*. New York: Oxford University Press.
- Braitenberg, V. (1984). *Vehicles: Experiments in synthetic psychology*. Cambridge, MA: MIT Press.
- Byl, K., & Tedrake, R. (2009). Metastable walking machines. *International Journal of Robotics Research*, 28(8), 1040–1064.
- Chevallereau, C., Abba, G., Aoustin, Y., Plestan, F., Westervelt, E. R., & Canudas-De-Wit, C. et al (2003). RABBIT: A testbed for advanced control theory. *IEEE Control Systems Magazine*, 23(5), 57–79.
- Chew, C. M., & Pratt, G. A. (2002). Dynamic bipedal walking assisted by learning. *Robotica*, 20, 477–491.
- Collins, S. H., & Ruina, A. (2005). *A Bipedal Walking Robot with Efficient and Human-Like Gait*. Paper presented at the Proceedings of the 2005 International Conference on Robotics and Automation, Barcelona, Spain.
- Collins, S. H., Ruina, A., Tedrake, R., & Wisse, M. (2005). Efficient bipedal robots based on passive-dynamic walkers. *Science*, 307, 1082–1085.
- Eiben, A., & Smith, J. (2003). *Introduction to evolutionary computing* (1st ed.). Heidelberg: Springer.
- Endo, E., Morimoto, J., Nakanishi, J., & Cheng, J. (2004). *An Empirical Exploration of a Neural Oscillator for Biped Locomotion Control*. Paper presented at the Proceedings of the 2004 IEEE International Conference on Robotics & Automation, New Orleans, LA, USA.
- Garcia, M., Chatterjee, A., Ruina, A., & Coleman, M. (1998). The simplest walking model: Stability, complexity, and scaling. *Journal of Biomechanical Engineering*, 120(2), 281–288.
- Goswami, A., Espiau, B., & Keramane, A. (1996). *Limit Cycles and Their Stability in a Passive Bipedal Gait*. Paper presented at the Proceedings of the 1996 IEEE International Conference on Robotics and Automation, Minneapolis, MN, USA.
- Hobbelen, D. G. E., & Wisse, M. (2007). Limit cycle walking. In M. Hackel (Ed.), *Humanoid robots*. Vienna: I-Tech Education and Publishing.
- Hobbelen, D. G. E., & Wisse, M. (2008a). Ankle actuation for limit cycle walkers. *The International Journal of Robotics Research*, 27(6), 709–735.
- Hobbelen, D. G. E., & Wisse, M. (2008b). Controlling the walking speed in limit cycle walking. *The International Journal of Robotics Research*, 27(9), 989–1005.
- Hobbelen, D. G. E., & Wisse, M. (2008c). Swing leg retraction for limit cycle walkers improves disturbance rejection. *IEEE Transactions on Robotics*, 24(2), 377–389.
- Hobbelen, D. G. E., & Wisse, M. (2009). Active lateral foot placement for 3D stabilization of a limit cycle walker prototype. *International Journal of Humanoid Robotics*, 6(1), 93–116.
- Hobbelen, D. G. E., & Wisse, M. (2010). *Upper body feedback and feedforward control in limit cycle walkers*. Manuscript submitted for publication.
- Ishida, T. (2004). Development of a small biped entertainment robot QRIO. *Proceedings of the International Symposium on Micro-Nanomechanics and Human Science*, pp. 23–28.
- Jakobi, N., Husbands, P., & Harvey, I. (1995). *Noise and the Reality Gap: The Use of Simulation in Evolutionary Robotics*. Paper presented at the Advances in Artificial Life: Proceedings of the 3rd European Conference on Artificial Life.
- Kuo, A. D. (1999). Stabilization of lateral motion in passive dynamic walking. *International Journal of Robotics Research*, 18(9), 917–930.
- Kuo, A. D. (2002). Energetics of actively powered locomotion using the simplest walking model. *Journal of Biomechanical Engineering*, 124, 113–120.
- Manoonpong, P., Geng, T., Kulvicius, T., Porr, B., & Wörgötter, F. (2007). Adaptive, fast walking in a biped robot under neuronal control and learning. *PLoS Computational Biology*, 3(7), 1–15.
- McGeer, T. (1990). Passive dynamic walking. *The International Journal of Robotics Research*, 9(2), 62–82.
- McHale, G., & Husbands, P. (2004). *GasNets and Other Evolvable Neural Networks Applied to Bipedal Locomotion*. Paper presented at the From Animals to Animats 8: Proceedings of the 8th International Conference on Simulation of Adaptive Behavior.
- Mondada, F., & Floreano, D. (1995). Evolution of neural control structures: Some experiments on mobile robots. *Robotics and Autonomous Systems*, 16, 183–195.
- Ono, K., Takahashi, R., & Shimada, T. (2001). Self-excited walking of a biped mechanism. *The International Journal of Robotics Research*, 20(12), 953–966.
- Paul, C. (2005). Sensorimotor control of biped locomotion. *Adaptive Behavior*, 13(1), 67–80.
- Pratt, J. E. (2000). *Exploiting inherent robustness and natural dynamics in the control of walking robots*. Cambridge, MA: Unpublished doctoral dissertation, Massachusetts Institute of Technology.
- Reil, T., & Husbands, P. (2002). Evolution of central pattern generators for bipedal walking in a real-time physics environment. *IEEE Transactions on Evolutionary Computation*, 6(2), 159–168.
- Sakagami, Y., Wantanabe, R., Aoyama, C., Matsunaga, S., Higaki, N., & Fujita, M. (2002). *The Intelligent ASIMO: System Overview and Integration*. Paper presented at the Proceedings of the International Conference on Intelligent Robots and Systems.
- Schuitema, E., Hobbelen, D. G. E., Jonker, P. P., Wisse, M., & Karssen, J. G. D. (2005). *Using a Controller Based on Reinforcement Learning for a Passive Dynamic Walking Robot*. Paper presented at the Proceedings of 2005 5th IEEE-RAS International Conference on Humanoid Robots.
- Stefano, N., & Floreano, D. (2000). *Evolutionary robotics: The biology, intelligence, and technology of self-organizing machines*. Cambridge, MA: MIT Press.
- Strogatz, S. H. (2000). *Nonlinear dynamics and control*. Cambridge, MA: Westview Press.

- Taga, G., Yamaguchi, Y., & Shimizu, H. (1991). Self-organized control of bipedal locomotion by neural oscillators in unpredictable environment. *Biological Cybernetics*, 65, 147–159.
- Taga, G. (1995a). A model of the neuro-musculo-skeletal system for human locomotion: I. Emergence of basic gait. *Biological Cybernetics*, 37, 97–111.
- Taga, G. (1995b). A model of the neuro-musculo-skeletal system for human locomotion: II. Real-time adaptability under various constraints. *Biological Cybernetics*, 37, 113–121.
- Tedrake, R., Zhang, T. W., & Seung, H. S. (2004). Stochastic policy gradient reinforcement learning on a simple 3D biped. Proceedings of the 2004 IEEE/RSJ International Conference on Intelligent Robots and Systems, September 28–October 2, 2004, Sendai, Japan.
- Vaughan, E. D., Di Paolo, E., & Harvey, I. R. (2004). *The Evolution of Control and Adaptation in a 3D Powered Passive Dynamic Walker*. Paper presented at the Proceedings of the 9th International Conference on the Simulation and Synthesis of Living Systems, Boston, MA, USA.
- Vukobratović, M., & Borovac, B. (2004). Zero-moment point – thirty years of its life. *International Journal of Humanoid Robotics*, 1(1), 157–173.
- Winter, D. A. (1991). *The biomechanics and motor control of human gait*. Waterloo, ON, Canada: University of Waterloo Press.
- Wisse, M. (2005). Three additions to passive dynamic walking: Actuation, an upper body, and 3D stability. *International Journal of Humanoid Robotics*, 2(4), 459–478.
- Wisse, M., Hobbelen, D. G. E., Rotteveel, R. J. J., Anderson, S. O., & Zeglin, G. J. (2006). *Ankle Springs Instead of Arc-Shaped Feet for Passive Dynamic Walkers*. Paper presented at the Proceedings of the 2006 IEEE International conference on Humanoid Robots.
- Wisse, M., Schwab, A. L., van der Linde, R. Q., & van der Helm, F. C. T. (2005). How to keep from falling forward; elementary swing leg action for passive dynamic walkers. *IEEE Transactions on Robotics*, 21(3), 393–401.

About the Authors



Joseph H. Solomon is currently a postdoctoral scholar with the Mechanical Engineering Department at Northwestern University, Evanston, IL. He received a B.S. degree in aeronautical and astronautical engineering from the University of Illinois at Urbana-Champaign in 2001, an M.S. degree in mechanical engineering from the University of Illinois at Chicago in 2003, and a Ph.D. degree in mechanical engineering from Northwestern University in 2008. His research interests include evolutionary robotics, neural networks, artificial general intelligence, biomimetic sensing, and bipedal locomotion. He is a member of the American Association for the Advancement of Science.



Martijn Wisse is an associate professor at the Department of Mechanical Engineering, Delft University of Technology, The Netherlands. He received an M.S. degree (2000) and Ph.D. degree (2004) from Delft University of Technology on the topic of natural dynamic bipedal walking robots. In 2004–2005, he had a postdoctoral position at the Robotics Institute of Carnegie Mellon University. Dr Wisse is a member of IEEE. *Address:* Department of Mechanical Engineering, Delft University of Technology, 2628CD Delft, The Netherlands. *E-mail:* m.wisse@tudelft.nl.



Mitra J. Z. Hartmann is an associate professor at Northwestern University with a 50/50 joint appointment between the departments of Biomedical Engineering and Mechanical Engineering. She received a B.S. degree in applied and engineering physics from Cornell University, and a Ph.D. degree in integrative neuroscience from the California Institute of Technology. From 2000–2003, she was a postdoctoral scholar at the Jet Propulsion Laboratory in Pasadena, California, where she worked in the Bio-Inspired Technology and Systems group. Dr Hartmann is a member of the Biomedical Engineering Society, the American Society of Mechanical Engineers, the Society for Neuroscience, and the Society of Women Engineers. *Address:* Departments of Biomedical and Mechanical Engineering, Northwestern University, Evanston, IL 60208, USA. *E-mail:* m-hartmann@northwestern.edu.

Appendix: Normalization of State Variables

When training neural networks, it is good practice to normalize the input variables according their expected range of values (Bishop, 1996). In the present work, reasonable estimates could be made for the ranges of joint angles, but it was more difficult to establish estimates for the ranges of joint velocities. Therefore, a preliminary EA run without input variable scaling was made using Model 4. A reasonably stable controller evolved, and the variable limits were based on its behavior over a single 100 m walk, shown in Table A1. Using these values, all variables were affinely transformed to the range $[-1, 1]$ for the experiments described in Section 3.

Table A1. Ranges used to normalize state variables. Units are [rad] or [rad/s]

	$\phi_{h,st}$	$\phi_{h,sw}$	$\phi_{k,sw}$	ϕ_{il}
min	-0.448	-0.197	0	-0.571
max	0.157	0.458	0.434	0.582
	$\dot{\phi}_{h,st}$	$\dot{\phi}_{h,sw}$	$\dot{\phi}_{k,sw}$	$\dot{\phi}_{il}$
min	-1.652	-3.273	-4.813	-3.575
max	0.887	0.320	4.459	-0.111